

E4-2011-107

A. P. Severyukhin, V. V. Voronov, Nguyen Van Giai*

SPIN-ISOSPIN EXCITATIONS IN NUCLEI
AND A SEPARABLE APPROXIMATION
FOR SKYRME INTERACTIONS

Talk at the KLFTP-BLTP Joint Workshop on Nuclear Physics,
September 6–8, 2011, Institute of Theoretical Physics, Chinese Academy
of Sciences, Beijing, China

*Institut de Physique Nucléaire, CNRS-IN2P3 and University Paris-Sud,
Orsay, France

Северюхин А. П., Воронов В. В., Нгуен Ван Джай
Спин-изоспиновые возбуждения в ядрах и сепарабельная
аппроксимация взаимодействия Скирма

E4-2011-107

Сепарабельная аппроксимация сил Скирма применена к изучению зарядово-обменных возбуждений в сферических ядрах. Эта аппроксимация позволяет заметно сократить размерности матриц, которые диагонализуются в расчетах квазичастичного приближения случайных фаз в больших конфигурационных пространствах. Возможности метода продемонстрированы на примере распределений сил гамов-теллеровских и спин-дипольных переходов в ядрах ^{90}Zr , ^{132}Sn , $^{126,128,130}\text{Cd}$. Результаты расчетов находятся в согласии с существующими экспериментальными данными.

Работа выполнена в Лаборатории теоретической физики им. Н. Н. Боголюбова ОИЯИ.

Препринт Объединенного института ядерных исследований. Дубна, 2011

Severyukhin A. P., Voronov V. V., Nguyen Van Giai
Spin–Isospin Excitations in Nuclei and a Separable Approximation
for Skyrme Interactions

E4-2011-107

A finite rank separable approximation of Skyrme forces is applied to study charge-exchange excitations in spherical nuclei. This approximation enables one to reduce considerably the dimensions of the matrices that must be diagonalized to perform QRPA calculations in large configuration spaces. Choosing as examples the nuclei ^{90}Zr , ^{132}Sn and $^{126,128,130}\text{Cd}$, we demonstrate an ability of the method to study the Gamow–Teller and spin-dipole strength distributions. It is shown that characteristics calculated within the approach are in a reasonable agreement with available experimental data.

The investigation has been performed at the Bogoliubov Laboratory of Theoretical Physics, JINR.

Preprint of the Joint Institute for Nuclear Research. Dubna, 2011

INTRODUCTION

A study of the charge-exchange nuclear modes is an interesting problem not only from the nuclear structure point of view, but it is very important for the nuclear astrophysics applications. Many versions of the self-consistent approach based on the Random Phase Approximation (RPA) or the quasiparticle RPA (QRPA) were developed during last years, see, for example, [1–10]. A comparison of such calculations with recent experimental data demonstrates that model mentioned above cannot reproduce correctly the strength distribution of the spin–isospin resonances. It is necessary to take into account a coupling with more complex configurations that results in shifting some strength up [11–13]. Moreover, the tensor forces can give an additional shift [10, 11]. It is much simpler to include a coupling in QRPA calculations if one uses separable forces [12–14]. This idea stimulated us to develop the finite rank separable approximation (FRSA) for the Skyrme interactions [15, 16] that enables one to perform calculations in the large configuration space. Applications of our method to study the low-lying states and giant resonances within the QRPA and beyond are given in [15–18]. Recently, we have proposed an extension of our approach for the charge-exchange nuclear excitations [19–21]. Before to investigate effects of the coupling we need to be sure that the finite rank approximation for the Skyrme interactions is good enough to reproduce main characteristics of such nuclear modes.

In this work we describe briefly our method for the charge-exchange excitations and present our investigations of properties of the Gamow–Teller (G–T) resonances and the spin-dipole (SD) resonances in some spherical nuclei.

1. THE METHOD

The starting point of the method is the HF–BCS calculation [22] of the parent ground state, where spherical symmetry is imposed on the quasiparticle wave functions. The continuous part of the single-particle spectrum is discretized by diagonalizing the Skyrme HF Hamiltonian on a harmonic oscillator basis. We work in the quasiparticle representation defined by the canonical Bogoliubov transformation:

$$a_{jm}^+ = u_j \alpha_{jm}^+ + (-1)^{j-m} v_j \alpha_{j-m}, \quad (1)$$

where jm denote the quantum numbers $nljm$. We use the Skyrme interaction [23] in the p - h channel, while the pairing correlations are generated by the surface peaked density-dependent zero-range force

$$V_{\text{pair}}(\mathbf{r}_1, \mathbf{r}_2) = V_0 \left(1 - \frac{\rho(r_1)}{\rho_c} \right) \delta(\mathbf{r}_1 - \mathbf{r}_2). \quad (2)$$

Here $\rho(r_1)$ is the particle density in the coordinate space, ρ_c is equal to the nuclear saturation density, the strength V_0 is the parameter fixed to reproduce the odd-even mass difference of nuclei in the study region. In order to avoid divergences, it is necessary to introduce a cutoff in the single-particle space. This cutoff limits the active pairing space above the Fermi level. We used a procedure that is proposed in [16, 24].

The residual interaction in the p - h channel V_{res} can be obtained as the second derivative of the energy density functional with respect to the particle density ρ . Following our previous paper [15], we simplify V_{res} by approximating it by its Landau–Migdal form. For Skyrme interactions all Landau parameters with $l > 1$ are zero and they are functions of the coordinate \mathbf{r} . We keep only the $l = 0$ terms in V_{res} and the expressions for F'_0, G'_0 in terms of the Skyrme force parameters can be found in [25]. The Coulomb and spin-orbit residual interactions are dropped. Therefore, we can write the residual interaction in the isovector channel in the following form:

$$V_{\text{res}}(\mathbf{r}_1, \mathbf{r}_2) = N_0^{-1} [F'_0(r_1) + G'_0(r_1) \boldsymbol{\sigma}^{(1)} \cdot \boldsymbol{\sigma}^{(2)}] \boldsymbol{\tau}^{(1)} \boldsymbol{\tau}^{(2)} \delta(\mathbf{r}_1 - \mathbf{r}_2), \quad (3)$$

where $\boldsymbol{\sigma}^{(i)}$ and $\boldsymbol{\tau}^{(i)}$ are the spin and isospin operators, and $N_0 = 2k_F m^* / \pi^2 \hbar^2$ with k_F and m^* standing for the Fermi momentum and nucleon effective mass in nuclear matter.

In what follows we use the second quantized representation and \hat{V}_{res} can be written as

$$\hat{V}_{\text{res}} = \frac{1}{4} \sum_{1234} (V_{1234} - V_{1243}) : a_1^\dagger a_2^\dagger a_4 a_3 := \hat{V}_M + \hat{V}_{SM}, \quad (4)$$

where $a_1^\dagger (a_1)$ is the particle creation (annihilation) operator and 1 denotes quantum numbers (n_1, l_1, j_1, m_1) . Following our method [15–18], the residual interactions can be reduced to a finite rank separable form:

$$\hat{V}_M = -2 \sum_{JM} \sum_{k=1}^N \kappa_F^{(k)} : \hat{M}_{JM}^{(k)+} \hat{M}_{JM}^{(k)} :, \quad (5)$$

$$\hat{V}_{SM} = -2 \sum_{JM} \sum_{L=J; J\pm 1} \sum_{k=1}^N \kappa_G^{(k)} : \hat{S}_{LJM}^{(k)+} \hat{S}_{LJM}^{(k)} :, \quad (6)$$

$$\begin{pmatrix} \kappa_F^{(k)} \\ \kappa_G^{(k)} \end{pmatrix} = -N_0^{-1} \frac{Rw_k}{2r_k^2} \begin{pmatrix} F_0'(r_k) \\ G_0'(r_k) \end{pmatrix}, \quad (7)$$

where R is a large enough cutoff radius for a N -point integration Gauss formula with abscissas r_k and weights w_k [15].

The operators entering the normal products in Eqs. (5), (6) are defined as follows:

$$\begin{aligned} \hat{M}_{JM}^{(k)+} &= (-1)^{J-M} \hat{J}^{-1} \sum_{j_n j_p m_n m_p} \langle j_n m_n j_p - m_p | JM \rangle \times \\ &\quad \times f_{j_n j_p}^{(Jk)} (-1)^{j_p - m_p} a_{j_n m_n}^+ a_{j_p m_p}, \quad (8) \end{aligned}$$

$$\begin{aligned} \hat{S}_{LJM}^{(k)+} &= (-1)^{J-M} \hat{J}^{-1} \sum_{j_n j_p m_n m_p} \langle j_n m_n j_p - m_p | JM \rangle \times \\ &\quad \times g_{j_n j_p}^{(LJk)} (-1)^{j_p - m_p} a_{j_n m_n}^+ a_{j_p m_p}. \quad (9) \end{aligned}$$

$f_{j_n j_p}^{(Jk)}$ are the single-particle matrix elements of the multipole operators,

$$f_{j_n j_p}^{(Jk)} = u_{j_n}(r_k) u_{j_p}(r_k) \langle j_n || i^J Y_J || j_p \rangle, \quad (10)$$

and $g_{j_n j_p}^{(LJk)}$ are the single-particle matrix elements of the spin-multipole operators,

$$g_{j_n j_p}^{(LJk)} = u_{j_n}(r_k) u_{j_p}(r_k) \langle j_n || i^L T_{LJ} || j_p \rangle. \quad (11)$$

In the above equations, $\langle j_n || i^J Y_J || j_p \rangle$ is the reduced matrix element of the spherical harmonics Y_{JM} , $\hat{J} = \sqrt{2J+1}$, $T_{LJM}(\hat{r}, \sigma) = [Y_L \times \sigma]_J^M$. The radial wave functions $u_j(r)$ are related to the HF single-particle wave functions,

$$\phi_{i,m}(1) = \frac{u_i(r_1)}{r_1} \mathcal{Y}_{l_i, j_i}^m(r_1, \sigma_1). \quad (12)$$

We introduce the phonon creation operators

$$Q_{JM}^+ = \sum_{j_n j_p} (X_{j_n j_p}^{Ji} A^+(j_n j_p; JM) - (-1)^{J-M} Y_{j_n j_p}^{Ji} A(j_n j_p; J-M)), \quad (13)$$

$$A^+(j_n j_p; JM) = \sum_{m_n m_p} \langle j_n m_n j_p m_p | JM \rangle \alpha_{j_n m_n}^+ \alpha_{j_p m_p}^+, \quad (14)$$

where the index J denotes total angular momentum and M is its z -projection in the laboratory system. One assumes that the ground state is the QRPA phonon vacuum $|0\rangle$ and the excited states are defined as $Q_{JM}^+ |0\rangle$. Making use of the

linearized equation-of-motion approach one can get the QRPA equations [22]:

$$\begin{pmatrix} \mathcal{A} & \mathcal{B} \\ -\mathcal{B} & -\mathcal{A} \end{pmatrix} \begin{pmatrix} X \\ Y \end{pmatrix} = \omega \begin{pmatrix} X \\ Y \end{pmatrix}. \quad (15)$$

The $\mathcal{A}_{(j_n j_p)(j'_n j'_p)}^J$ matrix is related to forward-going graphs and the $\mathcal{B}_{(j_n j_p)(j'_n j'_p)}^J$ matrix is related to backward-going graphs. The dimension of the matrices \mathcal{A}, \mathcal{B} is the space size of the two-quasiparticle configurations. The explicit solution of the corresponding QRPA equations is described in detail elsewhere [21]. Our approach enables one to reduce remarkably the dimensions of the matrices that must be inverted to perform nuclear structure calculations in very large configuration spaces. It is shown that the matrix dimensions never exceed $4N \times 4N$ independently of the configuration space size. Our previous study of the FRSA applied to charge-exchange excitations [21] enables us to conclude that a value $N = 45$ for the number of Gauss points in the radial integrals is sufficient for the desired accuracy in all nuclei with $A \leq 208$.

The excitation energies with respect to the parent ground state are

$$E_{Ji}^{\mp} = \omega_{Ji} \mp (\lambda_n - \lambda_p), \quad (16)$$

where ω_{Ji} denotes the QRPA energies in the T_{\mp} channels, λ_n and λ_p being the neutron and the proton chemical potentials, respectively.

2. RESULTS

First, we show the accuracy of the FRSA by comparing results obtained using this separable approximation with those from a full treatment of the Skyrme-type p - h residual interaction. We select the SD transitions in the T_- and T_+ channels from the parent ground states of ^{90}Zr and ^{132}Sn as illustrative cases. For the sake of simplicity the check is done within the Tamm–Dancoff approximation (TDA) without pairing effects. The RPA results would be similar because the backward-going graphs are somewhat blocked in these charge-exchange channels, and in any case we are just interested here in assessing the validity of the FRSA.

In this work, the calculations are done with the Skyrme parameter set SGII [25] which was designed to give reasonable values for the spin–isospin Landau parameters ($G_0 = 0.01$, $G'_0 = 0.50$ at saturation density). The HF mean field is first calculated in coordinate space, then the single-particle spectra necessary for the TDA calculations (energies and wave functions) are obtained by diagonalizing the HF mean field in a 12-shells harmonic oscillator basis and keeping all states below 100 MeV. This is sufficient to exhaust the Ikeda sum rule $3(N - Z)$ [26] for the G–T strength as well as the SD sum rule [27, 28]:

$$S_- - S_+ = \frac{9}{4\pi} (N \langle r^2 \rangle_n - Z \langle r^2 \rangle_p), \quad (17)$$

where

$$S_{\mp} = \sum_{\nu} |\langle N, Z | \hat{O}_{\mp} | N \mp 1, Z \pm 1; \nu \rangle|^2 \quad (18)$$

are the total SD transition strengths to the neighbouring daughter nuclei induced by the operators

$$\hat{O}_{\mp} = \sum_{i,m,\mu} r_i t_{\mp}(i) \sigma_m(i) Y_1^{\mu}(\hat{r}_i). \quad (19)$$

All calculations are without any quenching factor. In the figures, the calculated strength distributions are folded out with a Lorentzian distribution of 1 MeV width.

We compare the SD sum rule (17) calculated in FRSA and with the full SGII force [21]. To compare our calculations with experimental data in ^{90}Zr we choose the energy interval $E \leq 50$ MeV for the T_- channel and $E \leq 26$ MeV for the T_+ channel [7, 28]. The FRSA sum rules are quite close to those of the full calculations. The calculated values S_-, S_+ agree well with experimental data [7, 28] in ^{90}Zr . The SD sum rule (17) is an integral characteristic and it is less sensitive to the details than the SD strength distribution. The calculated T_- and T_+ strength distributions in various J^{π} channels are shown in Figs. 1 and 2, for the ^{90}Zr case. The excitation energies refer to the ground state of the parent nucleus ^{90}Zr . The experimental strength distributions [7, 28] for the T_- and T_+ channels are results of the multipole decomposition analysis done for the $^{90}\text{Zr}(p, n)^{90}\text{Nb}$ and $^{90}\text{Zr}(n, p)^{90}\text{Y}$ reactions, respectively. From Figs. 1 and 2, it can be seen that the FRSA reproduces the essential features of the SD strength distributions with a downward shift about 0.9 MeV in the positions of the high energy peaks for the T_- and T_+ channels. Thus, the p - h interaction in the FRSA is slightly weaker than the original interaction. The difference between the full calculation and the FRSA is small in global comparison with the experimental data. There is the missing of significant part of the experimental strength distribution in the region above the main peaks. One can expect a redistribution of strength if the coupling of the $1p$ - $1h$ configurations to more complex $2p$ - $2h$ configurations is taken into account [11, 13, 29]. The p - h interaction of the form Eqs. (5), (6) allows one to simplify the calculation of such couplings, and this study is now in progress. It is worth mentioning that the SD strength distributions in ^{90}Zr are rather well studied within the $1p$ - $1h$ configuration space (for example, see [6, 7, 9]). The effect of the tensor correlations on the SD strength distributions is studied in [30].

We have done a similar check of the FRSA in the case of the parent nucleus ^{132}Sn . A perfect agreement is obtained between the r.h.s. of Eq. (17) and the l.h.s. calculated either in FRSA or full Skyrme TDA [21]. The SD strength distributions summed over the three J^{π} components in both T_- and T_+ channels are shown in Fig. 3. As can be seen from Fig. 3, the FRSA treatment changes slightly the

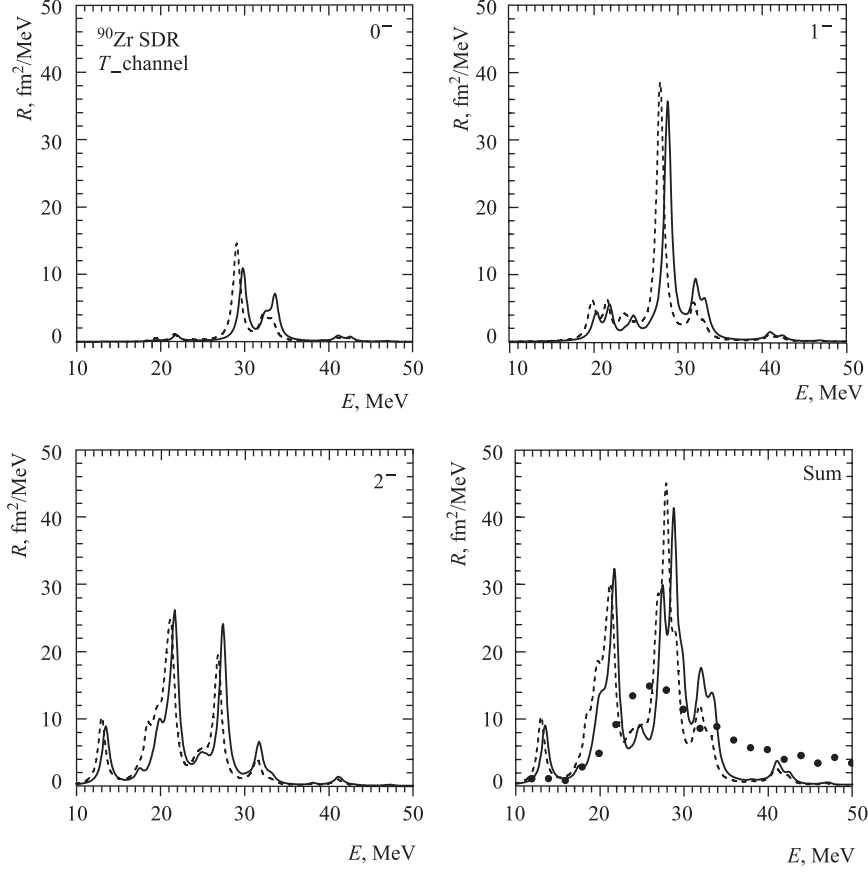


Fig. 1. Spin-dipole strength distributions in the T_- channel of the parent nucleus ^{90}Zr . The results with the FRSA for the $p-h$ interaction (dashed lines), and with the full $p-h$ interaction (solid lines) are shown. The black dots correspond to the experimental data

energies of the peaks in ^{132}Sb . However, we find that the general structure remains the same. The two low-lying peaks are due to the 2^- excitations. The main configuration of the peak at $E = 2.0$ MeV (1.5 MeV in the FRSA case) is $\left\{ \pi 1g \frac{7}{2} \nu 1h \frac{11}{2}^{-1} \right\}$. At the same time, the leading contribution of the peak at $E = 9.1$ MeV (8.8 MeV in FRSA) comes from the configuration $\left\{ \pi 1h \frac{11}{2} \nu 1g \frac{7}{2}^{-1} \right\}$. The peak around $E = 17.9$ MeV is related with the collective 0^- , 1^- , and 2^- states. The peak energy is moved downward by about 0.5 MeV in FRSA. The

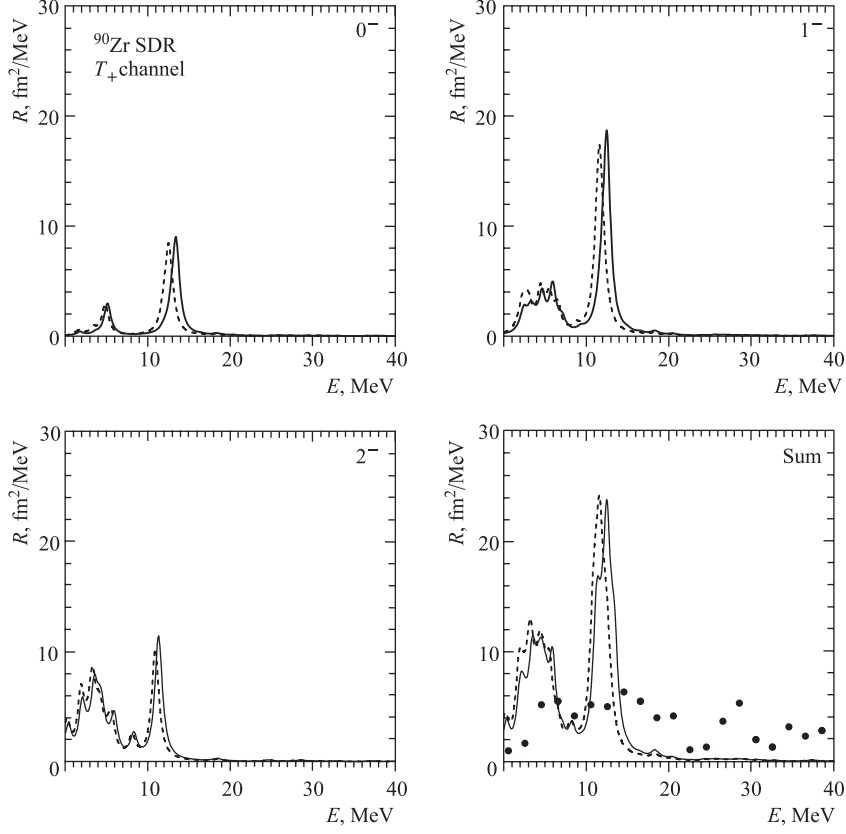


Fig. 2. The same as in Fig. 1, for the T_+ channel

main features of the high-energy broad bump are well reproduced by the FRSA. For the T_+ channel, the Pauli blocking of the neutron excess in ^{132}Sn is the reason why there is only one sharp peak in the strength distribution, and the S_+ value is much smaller than the S_- value. The $J^\pi = 0^-, 1^-,$ and 2^- states in the daughter nucleus ^{132}In are concentrated in the sharp peak at $E = 14.1$ MeV which is shifted downward by 0.5 MeV if one uses the FRSA. The 0^- and 1^- states are due to the $\left\{ \nu 1 h \frac{9}{2} \pi 1 g \frac{9^{-1}}{2} \right\}$ configuration. The main configurations of the 2^- state are the $\left\{ \nu 1 h \frac{9}{2} \pi 1 g \frac{9^{-1}}{2} \right\}$ and $\left\{ \nu 2 f \frac{5}{2} \pi 1 g \frac{9^{-1}}{2} \right\}$.

One can thus conclude that the FRSA can reliably be used for the study of charge-exchange modes in the ^{90}Zr as well as ^{132}Sn regions.

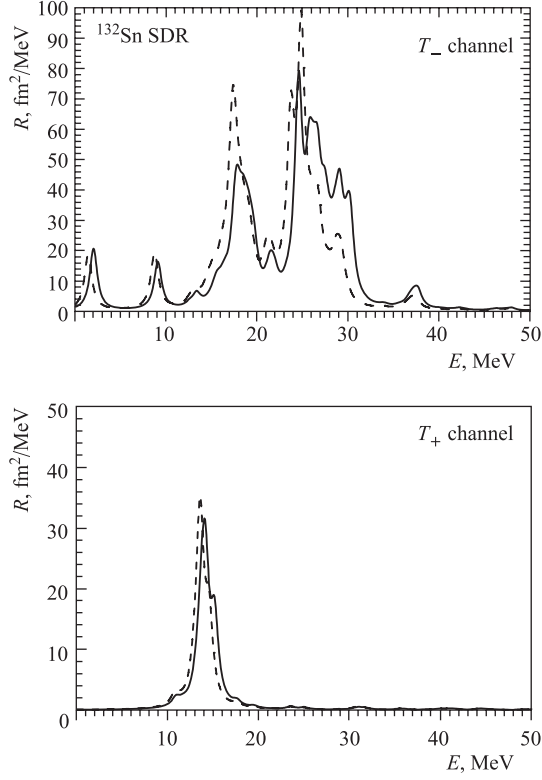


Fig. 3. The spin-dipole strength distributions summed over $J^\pi = 0^-, 1^-, 2^-$ in both T_\mp channels in ^{132}Sn . The same notations as in Figs. 1 and 2

There is a relation between the $N = 82$ shell closure and the $A \approx 130$ peak of the solar r-process abundance distribution [31]. The $N = 82$ isotones below ^{132}Sn are important for stellar nucleosynthesis, see, e.g., [32–35]. It is interesting to study the properties of the G–T and SD states in $^{126-130}\text{Cd}$ within the QRPA.

We use the isospin-invariant surface-peaked pairing force (2), with the value $\rho_0 = 0.16 \text{ fm}^{-3}$ of the nuclear saturation density corresponding to the SGII force. The strength $V_0 = -870 \text{ MeV fm}^3$ is fitted to reproduce the experimental pairing energies [21]. The definition of the pairing force (2) involves the energy cutoff of the single-particle space to restrict the active pairing space. We use the soft cutoff at 10 MeV above the Fermi energies as proposed in [16, 24].

Figure 4 shows the evolution of the G–T strength distributions in $^{126,128,130}\text{Cd}$. One can see that the major part of the strength is concentrated in the peaks at $E = 14.9, 14.3,$ and 13.8 MeV for $^{126}\text{Cd}, ^{128}\text{Cd},$ and ^{130}Cd , respectively. The

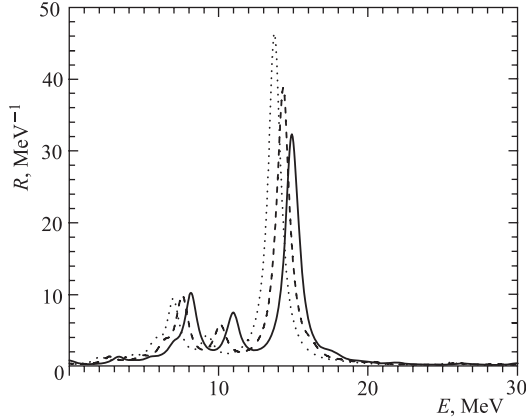


Fig. 4. The G–T strength distributions in ^{126}Cd (solid line), ^{128}Cd (dashed line), ^{130}Cd (dotted line)

largest contribution in the peaks comes from the configuration $\left\{ \pi 1h \frac{9}{2} \nu 1h \frac{11}{2} \right\}$. About 99% of the G–T strength distribution is located below 30 MeV with respect to the parent ground state. Taking into account the QRPA tensor correlations within our approach [37] can improve the results. The tensor correlations can shift up about 10% of the G–T strength to the higher energy region in the case of ^{90}Zr and ^{208}Pb [10, 36, 37].

The evolution of the SD strength in the T_- channel of the three J^π components is shown in Fig. 5. A comparison of the calculated SD sum rule with the right-hand side of Eq. (17) shows that the SD sum rule is exhausted with a good accuracy [21]. The slight increase in the S_- value and the noticeable decrease in the S_+ value when the mass number grows. It is worth mentioning that the ratio 5 : 3 : 1 of the three J^π components of the $S_- - S_+$ value is fulfilled in our calculations. As can be seen from Fig. 4, for the T_- channel the fragmentation of the SD strength distributions increases with the value of J . The distributions are shifted to lower energies as one goes from ^{126}Cd to ^{130}Cd . In particular, the peak energy of the $J^\pi = 0^-$ mode of the SDR is 26.4, 25.7, and 25.0 MeV in ^{126}Cd , ^{128}Cd , and ^{130}Cd , respectively, and many configurations contribute to these structures. For the 1^- excitations, the shift of the main sharp peak is about 1 MeV. At the same time, the contribution of the leading configuration $\left\{ \pi 2i \frac{11}{2} \nu 1h \frac{11}{2} \right\}$ is decreasing from 54% for ^{126}Cd to 45% for ^{130}Cd . The spectrum of the 2^- states is fragmented in a wide energy range. There are two peaks in the strength distribution at lower energies. These low-energy excitations are of noncollective nature. In all three nuclei, the lowest peak is mainly due to the

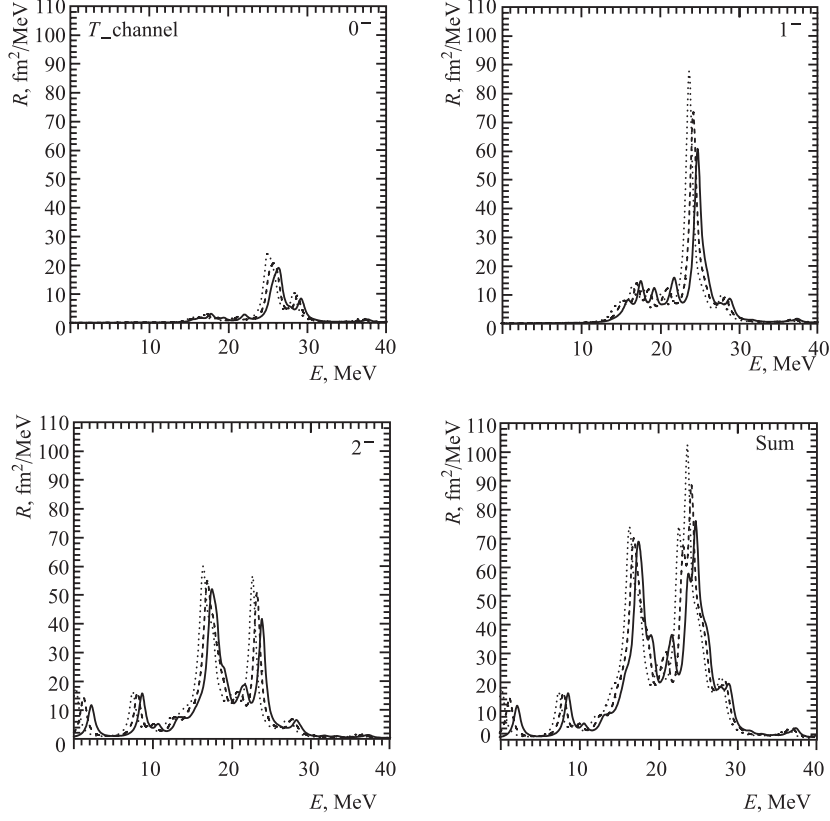


Fig. 5. Spin-dipole strength distributions of the T_- channel in ^{126}Cd (solid line), ^{128}Cd (dashed line), ^{130}Cd (dotted line)

configuration $\left\{ \pi 1g \frac{7}{2} \nu 1h \frac{11}{2} \right\}$, while the dominant configuration of the second one is $\left\{ \pi 1h \frac{11}{2} \nu 1g \frac{7}{2} \right\}$. It is worth pointing out that these configurations induce the low-energy peaks obtained in ^{132}Sn , as is discussed above. Most of the 2^- strength is concentrated in the two peaks around 17.5(16.4) and 23.8(22.6) MeV in ^{126}Cd (^{130}Cd). Thus, the three J^π modes of the SDR in $^{126,128,130}\text{Cd}$ keep to the energy hierarchy $E(2^-) < E(1^-) < E(0^-)$ as already found in ^{90}Zr [6, 7, 9].

The general behavior of the sharp peaks in the T_+ strength distribution is displayed in Fig. 6. With increasing mass number, the peak energy is moved upward from 14.0 MeV in ^{126}Cd to 14.8 MeV in ^{130}Cd . As expected, the Pauli blocking effect leads to a small contribution to the SD sum rule (17).

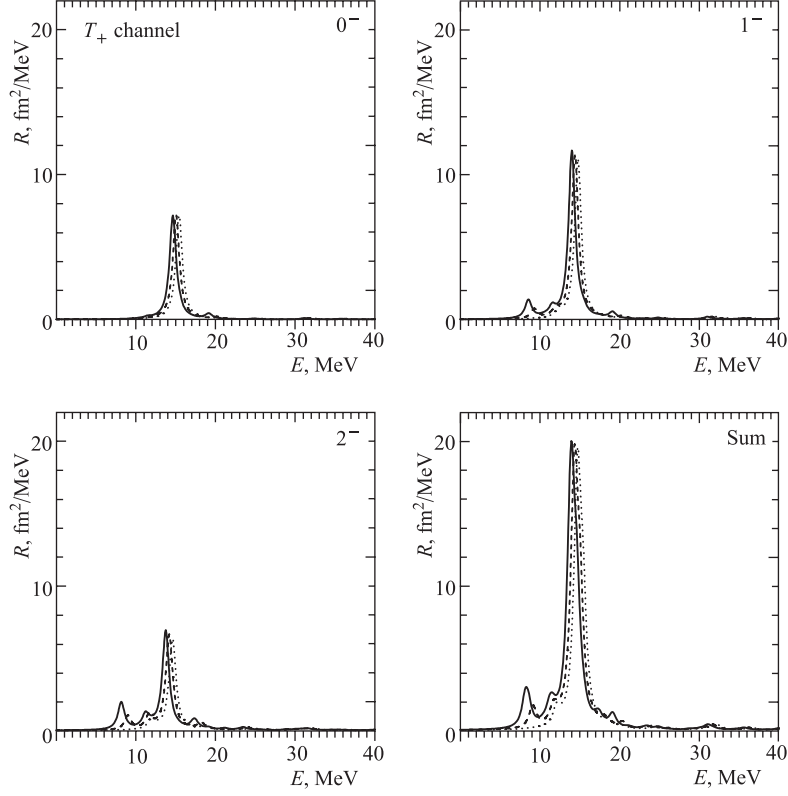


Fig. 6. The same as in Fig. 5, for the T_+ channel

The peaks in the 0^- and 1^- distributions have a noncollective structure with a dominant configuration $\left\{ \nu 1 h \frac{9}{2} \pi 1 g \frac{9}{2} \right\}$. In the case of the 2^- states, the leading configurations are $\left\{ \nu 2 f \frac{5}{2} \pi 1 g \frac{9}{2} \right\}$ and $\left\{ \nu 1 h \frac{9}{2} \pi 1 g \frac{9}{2} \right\}$. The situation is similar to the ^{132}Sn case. The structure peculiarities of the SD strength distributions are related with the shell structure in this region of nuclei.

CONCLUSION

A finite rank separable approximation of Skyrme-type forces, which was proposed in our previous work, is applied to study the charge-exchange nuclear modes. The suggested approach enables one to reduce remarkably the dimensions

of the matrices that must be inverted to perform nuclear structure calculations in very large configuration spaces.

As an illustration we present results of HF-TDA calculations for the Gamow–Teller and spin-dipole resonances in ^{90}Zr and ^{132}Sn . The values calculated within FRSA are very close to those that were calculated with the full Skyrme interaction. A comparison of our results with experimental data and other theoretical calculations demonstrates that the method gives a good description of properties of the charge-exchange excitations.

We have studied the G–T and spin-dipole strength distributions of the parent nuclei $^{126,128,130}\text{Cd}$ in the T_+ and T_- channels by performing QRPA calculations with the FRSA and the Skyrme parametrization SGII. Similarly to the case of ^{90}Zr we find that the peak energies of the spin-dipole distributions in these Cd isotopes obey the energy hierarchy $E(2^-) < E(1^-) < E(0^-)$.

An inclusion of the tensor terms of the Skyrme interaction and taking into account the coupling of the QRPA states with more complex components of the wave functions are in progress now.

Acknowledgements. We are grateful to H. Sagawa for valuable discussions. A. P. S. and V. V. V. thank IPN-Orsay, where a part of this work was done, for the hospitality. This work was partly supported by the IN2P3-JINR agreement No. 11-87 and the RFBR grant No. 110291054.

REFERENCES

1. Engel J. *et al.* // Phys. Rev. C. 1999. V. 60. P. 014302.
2. Khan E. *et al.* // Phys. Rev. C. 2002. V. 66. P. 024309.
3. Péru S., Berger J. F., Bortignon P. F. // Eur. Phys. J. A. 2005. V. 26. P. 25.
4. Vretenar D. *et al.* // Phys. Rep. 2005. V. 409. P. 101.
5. Terasaki J., Engel J. // Phys. Rev. C. 2006. V. 74. P. 044301.
6. Fracasso S., Colò G. // Phys. Rev. C. 2007. V. 76. P. 044307.
7. Sagawa H. *et al.* // Phys. Rev. C. 2007. V. 76. P. 024301.
8. Paar N. *et al.* // Rep. Prog. Phys. 2007. V. 70. P. 691.
9. Haozhao Liang, Nguyen Van Giai, Jie Meng // Phys. Rev. Lett. 2008. V. 101. P. 122502.
10. Bai C. L. *et al.* // Phys. Lett. B. 2009. V. 675. P. 28.
11. Bertsch G. F., Hamamoto I. // Phys. Rev. C. 1982. V. 26. P. 1323.
12. Kuzm̄in V. A., Soloviev V. G. // J. Phys. G. 1984. V. 10. P. 1507.
13. Kuzm̄in V. A., Soloviev V. G. // J. Phys. G. 1985. V. 11. P. 603.
14. Soloviev V. G. Theory of Atomic Nuclei: Quasiparticles and Phonons. Bristol; Philadelphia: Institute of Physics, 1992.
15. Nguyen Van Giai, Stoyanov Ch., Voronov V. V. // Phys. Rev. C. 1998. V. 57. P. 1204.

16. Severyukhin A. P., Voronov V. V., Nguyen Van Giai // Phys. Rev. C. 2008. V.77. P.024322.
17. Severyukhin A. P. et al. // Phys. Rev. C. 2002. V. 66. P.034304.
18. Severyukhin A. P., Voronov V. V., Nguyen Van Giai // Eur. Phys. J. A. 2004. V.22. P. 397.
19. Severyukhin A. P., Arsenyev N. N., Voronov V. V., Nguyen Van Giai // Phys. At. Nucl. 2009. V.72. P. 1149.
20. Severyukhin A. P., Voronov V. V., Nguyen Van Giai // J. Phys.: Conf. Ser. 2011. V.267. P.012025.
21. Severyukhin A. P., Voronov V. V., Nguyen Van Giai (in preparation).
22. Ring P., Schuck P. The Nuclear Many Body Problem. Berlin: Springer, 1980.
23. Vautherin D., Brink D. M. // Phys. Rev. C. 1972. V. 5. P. 626.
24. Krieger S. J. et al. // Nucl. Phys. A. 1990. V. 517. P. 275.
25. Nguyen Van Giai, Sagawa H. // Phys. Lett. B. 1981. V. 106. P. 379.
26. Ikeda K., Fujii S., Fujita J. I. // Phys. Lett. 1963. V. 3. P. 271.
27. Krasznahorkay A. et al. // Phys. Rev. Lett. 1999. V. 82. P. 3216.
28. Yako K., Sagawa H. Sakai H. // Phys. Rev. C. 2006. V. 74. P.051303(R).
29. Dröżdż S. et al. // Phys. Lett. B. 1987. V. 189. P. 271.
30. Bai C. L. et al. // Phys. Rev. C. 2011. V. 83. P.054316.
31. Burbidge E. M. et al. // Rev. Mod. Phys. 1957. V. 29. P. 547.
32. Martínez-Pinedo G., Langanke K. // Phys. Rev. Lett. 1999. V. 83. P. 4502.
33. Dillmann I. et al. // Phys. Rev. Lett. 2003. V. 91. P. 162503.
34. Jungclaus A. et al. // Phys. Rev. Lett. 2007. V. 99. P. 132501.
35. Cuenca-García J. J. et al. // Eur. Phys. J. A. 2007. V. 34. P. 99.
36. Bai C. L. et al. // Phys. Rev. C. 2009. V. 79. P.041301(R).
37. Severyukhin A. P., Sagawa H. (in preparation).

Received on October 26, 2011.

Корректор *Т. Е. Попеко*

Подписано в печать 19.12.2011.

Формат 60 × 90/16. Бумага офсетная. Печать офсетная.

Усл. печ. л. 1,18. Уч.-изд. л. 1,59. Тираж 310 экз. Заказ № 57532.

Издательский отдел Объединенного института ядерных исследований
141980, г. Дубна, Московская обл., ул. Жолио-Кюри, 6.

E-mail: publish@jinr.ru

www.jinr.ru/publish/